

Magnetoresistance of three-constituent composites: Percolation near a critical line

Sergey V. Barabash,¹ David J. Bergman,^{1,2} and D. Stroud¹¹Department of Physics, The Ohio State University, Columbus, Ohio 43210²School of Physics and Astronomy, Raymond and Beverly Sackler Faculty of Exact Sciences, Tel Aviv University, Tel Aviv 69978, Israel

(Received 12 July 2001; published 15 October 2001)

Scaling theory, duality symmetry, and numerical simulations of a random network model are used to study the magnetoresistance of a metal/insulator/perfect conductor composite with a disordered columnar microstructure. The phase diagram is found to have a critical line which separates regions of saturating and nonsaturating magnetoresistance. The percolation problem which describes this line is a generalization of anisotropic percolation. We locate the percolation threshold and determine the values of the critical exponents $t_{\parallel}=t_{\perp}=s_{\parallel}=s_{\perp}=1.30\pm 0.02$, $\nu=4/3\pm 0.02$, which are the same as in two-constituent two-dimensional isotropic percolation. We also determine the exponents which characterize the critical dependence on magnetic field, and confirm numerically that ν is independent of anisotropy. We propose and test a complete scaling description of the magnetoresistance in the vicinity of the critical line.

DOI: 10.1103/PhysRevB.64.174419

PACS number(s): 75.80.+q, 73.63.-b, 81.90.+c

I. INTRODUCTION

Magnetotransport in composite conductors has attracted increased attention due to the discovery of new effects, like the appearance of nonsaturating magnetoresistance in a metal/insulator columnar composite (denoted by M/I), induced by the Hall effect in the M (i.e., the metallic) constituent.¹ This means that, even when the M constituent has no *intrinsic* magnetoresistance but only a Hall resistivity, an induced magnetoresistance appears in the mixture and continues to increase as \mathbf{B}^2 (\mathbf{B} is the applied magnetic field) *indefinitely* whenever the Hall-to-Ohmic resistivity ratio of that constituent is much greater than 1. By contrast, in a columnar composite of normal conductor and perfect conductor (denoted by M/S), while there also appears an induced magnetoresistance, it saturates when \mathbf{B} is comparably large.¹ Related new effects were also found in periodic microstructures of either the M/I type or the M/S type, where the induced magnetoresistance often exhibits a strong anisotropy.^{2,3}

In this paper, we study the magnetoresistance of three-constituent composites with a *random columnar microstructure*. Specifically, we analyze a composite consisting of cylindrical I and S inclusions, though not necessarily circular cylinders, in an M host film, with cylinder axes perpendicular to the film, and with both a magnetic field and a uniform macroscopic or volume-averaged electric current applied *in the film plane*. We assume that the M constituent has a Hall effect, with a Hall-to-transverse-Ohmic resistivity ratio $H \equiv \rho_{Hall}/\rho_{Ohmic} = \mu|\mathbf{B}|$, where μ is the Hall mobility. We are concerned with the effective resistivity tensor $\hat{\rho}_e$ of this system at *large* H ($\hat{\rho}_e$ is defined by $\langle \mathbf{E} \rangle = \hat{\rho}_e \langle \mathbf{J} \rangle$, where $\langle \mathbf{E} \rangle$ and $\langle \mathbf{J} \rangle$ are the volume averaged electric field and current density⁴).

This system might appear to be inherently three dimensional (3D), because the Hall effect will generate an electric field with a component perpendicular to the film even with an in-plane applied current. However, the electric field perpendicular to the film plane vanishes because of the colum-

nar S inclusions. Moreover, this 3D problem can be reduced¹ to that of calculating the effective conductivity of a *two-dimensional* (2D) composite of perfect insulator I with $\sigma_I = 0$, perfect conductor (or superconductor) S with $\sigma_S = \infty$, and anisotropic 2D metal M with conductivity tensor

$$\hat{\sigma}_M \equiv \begin{pmatrix} \sigma_{M,\perp} & 0 \\ 0 & \sigma_{M,\parallel} \end{pmatrix} = \frac{1}{\rho_M} \begin{pmatrix} \frac{1}{1+H^2} & 0 \\ 0 & \frac{1}{\lambda} \end{pmatrix}. \quad (1)$$

The conductivities $\sigma_{M,\parallel}$ and $\sigma_{M,\perp}$ correspond to the in-plane directions parallel and perpendicular to the applied magnetic field \mathbf{B} . This transformation underlies our further discussion. The form assumed for $\hat{\sigma}_M$ means that the M constituent remains an isotropic conductor, even in a magnetic field. This excludes “open orbit” conductors, but includes the possibility of some intrinsic magnetoresistance: In that case both the transverse and longitudinal Ohmic resistivities ρ_M and $\lambda\rho_M$ would depend upon \mathbf{B} . Our subsequent discussion will assume, for simplicity, that $\lambda = 1$ and ρ_M are both independent of \mathbf{B} , as would be the case if M were a free electron or free hole conductor. In that case, H is simply proportional to $|\mathbf{B}|$. The three-constituent problem in 2D, but with a scalar $\hat{\sigma}_M$, was treated previously in Ref. 5. Scaling and simulational studies, of magnetotransport in 3D, two-constituent M/I composites with a random isotropic microstructure, were also performed previously.⁶

II. MAGNETORESISTANCE AND PERCOLATION

The relation of this problem to percolation can be understood by considering very large H . In this limit, $\sigma_{M,\perp} \rightarrow 0$, and within the metallic constituent the in-plane current prefers to flow in the $\sigma_{M,\parallel}$ direction. For large enough volume fraction p_S of the S constituent and small enough volume fraction p_I of I , there always exist current paths between S grains that are everywhere parallel to the high-conductivity direction in M [cf. Fig. 1(a)]. Therefore, in this regime, at

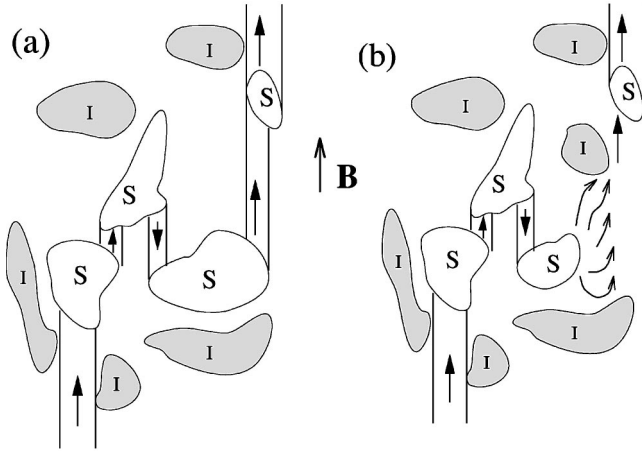


FIG. 1. Schematic of transport in a 2D composite of a perfect conductor S , insulator I , and a very anisotropic metal M (the host medium in this figure). The current prefers to flow between S grains only in the direction of high metallic conductivity $\sigma_{M,\parallel}$, i.e., parallel to \mathbf{B} . At high- S volume fraction p_S , such a path always exists, as shown schematically in (a). At smaller p_S or larger p_I , the current must sometimes flow through the metal in the low-conductivity direction ($\sigma_{M,\perp} \sim H^{-2}$), as shown in (b). This behavior leads to a nonsaturating effective resistivity.

large H the effective composite conductivity (and hence resistivity) saturates at some finite value. In the opposite case (small p_S , large p_I), the current will be forced in some regions to flow in the low-conductivity direction [cf. Fig. 1(b)]. In this case, the macroscopic or effective conductivity of the system will be proportional to $\sigma_{M,\perp}$. Hence, the effective resistivity ρ_e satisfies $\rho_e \sim 1/\sigma_{M,\perp} \sim H^2$; i.e., ρ_e will never saturate.

Next, we qualitatively discuss the expected “phase diagram” of this composite. The effective conductivity $\hat{\sigma}_e$ of the 2D mixture is a 2×2 tensor (like the effective 2D resistivity $\hat{\rho}_e = \hat{\sigma}_e^{-1}$), whose components depend on the applied magnetic field. If the in-plane microstructure is isotropic, then the principal axes of $\hat{\sigma}_e$ are determined by \mathbf{B} . At large H , both $\sigma_{e,\parallel}$ and $\sigma_{e,\perp}$ can either decrease as H^{-2} for arbitrarily large H or else saturate at some finite value. In principle, there could be a region in the phase diagram where the resistivity saturates along one principal axis, but not along the other. But we expect no such region in an infinite system. This conclusion, as well as the location of the critical line, follows from the relation between the present problem and the anisotropic percolation model in 2D, as we now explain.

Anisotropic percolation is usually defined in terms of a random resistor network (RRN), where the bond occupation probability depends on the bond orientation. In our 2D network model those probabilities will be chosen as $p_{\parallel} = p_M + p_S$ for bonds along \mathbf{B} , the high-conductivity direction of the M constituent, and $p_{\perp} = p_S$ for bonds perpendicular to \mathbf{B} , the low-conductivity direction. For an infinite network, the percolation threshold for both directions occurs when⁷ $1 = p_{\parallel} + p_{\perp} = 2p_S + p_M$, which implies

$$p_I = p_S. \quad (2)$$

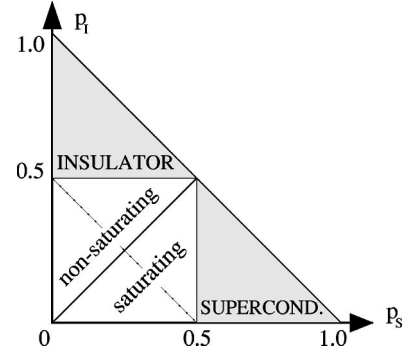


FIG. 2. Schematic phase diagram for an $M/I/S$ composite with random columnar microstructure. p_I and p_S are the volume fractions of I and S ; the M volume fraction is $p_M = 1 - p_I - p_S$. In the shaded regions, either the S or the I constituent percolates. The critical line $p_I = p_S$ separates regions with saturating and nonsaturating magnetoresistance. The dotted line corresponds to percolation of the metallic constituent alone ($p_M > 0.5$ or $p_I + p_S < 0.5$); no critical behavior appears to be associated with this line.

This threshold separates the regimes of saturating and nonsaturating magnetoresistance. It agrees with a prediction based on the effective medium approximation (EMA),^{8,9} as well as with numerical results below. In a composite with less symmetry between the I and S constituents, the threshold will usually differ from $p_I = p_S$.

The predicted phase diagram is shown in Fig. 2. For $p_S > 0.5$, the S constituent percolates; hence the composite is a perfect conductor. Similarly, if $p_I > 0.5$, then the combination of M and S constituents does not percolate; hence the composite is a perfect insulator. These behaviors are independent of how much of the M constituent is present. The remainder of the phase diagram is divided into saturating and nonsaturating regimes by the line $p_I = p_S$. In both regimes, our numerical results indicate that it is irrelevant whether the M constituent percolates by itself (as in the area below the dotted line) or whether only the aggregate of M and S constituents percolates.

III. CRITICAL EXPONENTS AND SCALING PROPERTIES

The critical behavior on approaching the critical line is described by a number of critical exponents. One of these governs the two correlation lengths ξ_{\parallel} and ξ_{\perp} , which diverge at the critical line. But we expect that the divergence of both will be governed by *the same* critical exponent ν , because their ratio $\xi_{\parallel}/\xi_{\perp}$ is determined by some function of the constituent volume fractions which remains finite on crossing the critical line.^{10,11} Thus we write

$$\xi_{\parallel} \sim \xi_{\perp} \sim (p_I - p_S)^{-\nu}. \quad (3)$$

Moreover, since the correlation length is just a geometrical property of a percolating system, it should have the same value ν_a as in anisotropic percolation, i.e., $\nu = \nu_a$. An earlier renormalization group analysis predicts that anisotropic percolation is governed by the isotropic fixed point.¹² We therefore expect that ν_a has the same value as in 2D isotropic percolation, which has been shown both analytically¹³ and

numerically¹⁴ to equal 4/3. However, a similar proof has not been given for anisotropic percolation;¹⁵ moreover, some time ago it was reported that ν does depend on anisotropy.¹⁶ Our numerical results below give $\nu=4/3\pm 0.02$, independent of anisotropy.

The magnetoresistance is described by other critical indices. At any point such that $p_I < p_S$ (the region below the critical line in Fig. 2), the effective conductivity saturates at some finite value ($i=\parallel$ or $i=\perp$):

$$g_{sat,i} \equiv \lim_{H \rightarrow \infty} \sigma_{sat,i}(H). \quad (4)$$

As we approach the critical line (say, along the line $p_M = \text{const}$), $g_{sat,i}$ must tend to 0, since on the other side of that line the conductivity vanishes at large H as H^{-2} . Hence we can introduce the critical exponents t_{\parallel} and t_{\perp} according to

$$g_{sat,i} \sim (p_S - p_I)^{t_i}. \quad (5)$$

In the region $p_I > p_S$, the effective conductivity is proportional to $1/H^2$. Therefore, we can define the finite limiting value

$$g_{nonsat,i} \equiv \lim_{H \rightarrow \infty} H^2 \sigma_{nonsat,i}(H). \quad (6)$$

Since $g_{nonsat,i}$ must diverge as the critical line is approached, we can define the critical exponents s_{\parallel} and s_{\perp} , according to

$$g_{nonsat,i} \sim (p_I - p_S)^{-s_i}. \quad (7)$$

Just as in the case of ν , we expect $s_{\parallel} = s_{\perp}$, $t_{\parallel} = t_{\perp}$. We might expect that the actual values of t and s are determined, once again, by the connection to anisotropic percolation. However, this connection is more subtle than for ν , because t and s refer to different physical quantities in the present problem than in anisotropic percolation. Nonetheless, it is reasonable to expect that both problems belong to the same universality class, implying $s_i = t_i = 1.30$, the values of the two conductivity exponents in conventional 2D percolation problems.¹⁷⁻¹⁹ Note also that the EMA yields $s_i = t_i = 1$,^{8,9} and that continuum composites sometimes belong to a different universality class of percolation, with different values of the critical exponents, depending upon the microstructural details.²⁰

Finally, consider systems exactly at the percolation threshold, i.e., at $p_I = p_S$. Any finite-size sample inevitably falls into either the percolating class, with $\rho_e \sim H^0$ as $H \rightarrow \infty$, or the nonpercolating class, with $\rho_e \sim H^2$. On increasing the size of the system, one finds that the field where a saturating sample achieves saturation also increases. The same size effect also holds for nonsaturating samples: the characteristic field at which ρ_e starts to vary as H^2 increases with the size of the system. Below that field, or at any field in the limit of a system of infinite size, the behavior of the magnetoresistance is described by yet another critical exponent δ_i , defined by

$$\rho_{e,i} \sim |H|^{\delta_i}. \quad (8)$$

The EMA analysis^{8,9} yields $\delta_i = 1$.

In fact, the result $\delta_i = 1$ also follows from a duality argument, if one assumes that $\delta_{\parallel} = \delta_{\perp}$. The duality principle⁴ gives

$$1 = \sigma_{e,\parallel}(\sigma_{M\parallel}, \sigma_{M\perp}, \sigma_S, \sigma_I) \sigma_{e,\perp} \left(\frac{1}{\sigma_{M\perp}}, \frac{1}{\sigma_{M\parallel}}, \frac{1}{\sigma_S}, \frac{1}{\sigma_I} \right).$$

It immediately follows that the anisotropic percolation thresholds for the two directions \parallel, \perp must coincide, for otherwise the singular behaviors of $\sigma_{e,\parallel}$ and $\sigma_{e,\perp}$ would not cancel, as required by this equation. It also follows, rigorously, that $t_{\parallel} = s_{\perp}$ and $t_{\perp} = s_{\parallel}$. Using the homogeneity of $\sigma_{e,\parallel}$, $\sigma_{e,\perp}$ as functions of the various constituent conductivities, and noting that $\sigma_I = 0$ and $\sigma_S = \infty$, we can rewrite this equation as

$$\frac{\sigma_{M\perp}}{\sigma_{M\parallel}} = \sigma_{e,\parallel} \left(1, \frac{\sigma_{M\perp}}{\sigma_{M\parallel}}, \infty, 0 \right) \sigma_{e,\perp} \left(1, \frac{\sigma_{M\perp}}{\sigma_{M\parallel}}, 0, \infty \right).$$

Note that the relation $p_I = p_S$ for the percolation threshold follows rigorously from this equation if the microstructure is invariant under the interchange of the S and I constituents. At the percolation threshold and when $|H| \gg 1$, this reduces to

$$\frac{1}{H^2} \propto \frac{1}{|H|^{\delta_{\parallel} + \delta_{\perp}}} \Rightarrow \delta_{\parallel} + \delta_{\perp} = 2.$$

The assumption that $\delta_{\parallel} = \delta_{\perp}$, and hence the final result $\delta_{\parallel} = \delta_{\perp} = 1$, is supported by the physical picture of the anisotropic percolation process and is consistent with the expectation that $t_{\parallel} = t_{\perp}$ and $s_{\parallel} = s_{\perp}$. These equalities also follow if a simple scaling description applies to both $\sigma_{e,\parallel}$ and $\sigma_{e,\perp}$ with *the same scaling variable*. Thus, for an $M/I/S$ columnar composite precisely at the critical composition (i.e., on the phase boundary line between saturating and nonsaturating magnetoresistance), we expect to find

$$\sigma_{e,\parallel} \sim \sigma_{e,\perp} \sim \frac{1}{|H|}, \quad \rho_{e,\parallel} \sim \rho_{e,\perp} \sim |H| \Rightarrow \delta = 1.$$

Near the transition, where $|p_I - p_S| \ll 1$ and $\sigma_{M,\perp} / \sigma_{M,\parallel} \equiv 1/H^2 \ll 1$, we expect that a scaling description of the critical behavior is applicable. In view of the preceding discussion, that description can be formulated as follows:

$$\frac{\rho_{e,i}}{\rho_{M,\parallel}} \equiv \text{sgn } \Delta p |\Delta p|^{-t} F_i(Z),$$

$$\Delta p \equiv p_I - p_S, \quad i = \parallel, \perp, \quad Z \equiv |H| |\Delta p|^t \text{sgn } \Delta p. \quad (9)$$

The scaling functions $F_i(Z)$ should have the following asymptotic forms for extreme values of the scaling variable Z :

$$F_i(Z) \sim \begin{cases} -Z^0 & \text{for } Z \ll -1, \quad \text{i.e., } p_S > p_I, \\ Z^2 & \text{for } Z \gg 1, \quad \text{i.e., } p_S < p_I, \\ Z & \text{for } |Z| \ll 1, \quad \text{i.e., } p_S \approx p_I. \end{cases} \quad (10)$$

The first two lines in this expression follow from the fact that we expect to have $\rho_{e,i} \sim H^0$ in the saturating regime and

$\rho_{e,i} \sim H^2$ in the nonsaturating regime. The third line results from the necessity to cancel the dependence of $\rho_{e,i}$ upon Δp when $\Delta p \rightarrow 0$. This kind of behavior was already found previously using the EMA,^{8,9} where the incorrect value $t=1$ was found, as is usual when that approximation is invoked. Note that, even though $F_i(Z)$ has a different analytic form for large Z , depending on the sign of Z or Δp , these functions are expected to vary smoothly when Z passes through 0.

Finally, note that duality is a general symmetry property of 2D systems, and does not require that the I and S inclusions have similar shapes or spatial distributions. Thus, the conclusions regarding values of s , t , δ are valid even if the line of critical compositions differs from the simple straight line $p_S = p_I$, which is valid only for the case where the I and S constituents appear in the composite in a symmetric fashion.

IV. NUMERICAL RESULTS

We carried out calculations on simple-square-lattice RRN's, choosing the resistors in accordance with the model described above. The calculation was done using the Y - Δ bond elimination algorithm.¹⁸ Besides being very efficient in 2D, this algorithm allows the inclusion of both perfectly insulating and perfectly conducting bonds without any approximations. This technique is much more efficient than the techniques available for 3D networks. That is why the results obtained here for columnar systems are much more detailed and accurate than the results obtained previously for 3D isotropic systems by simulations of 3D random network models.⁶

The networks for our results were constructed as follows: each bond was independently and randomly chosen to be insulating, perfectly conducting, or metallic, with appropriate probabilities. A metallic bond was assigned an appropriate conductance, depending on whether it was oriented parallel or perpendicular to the magnetic field. To calculate $g_{sat,i}$, as can be seen from Eqs. (1) and (4), the conductances of the constituents should be taken as

$$\sigma_I = 0, \quad \sigma_S = \infty, \quad \sigma_{M,\parallel} = 1, \quad \sigma_{M,\perp} = 0. \quad (11)$$

But in order to calculate $g_{nonsat,i}$, one needs to multiply all the conductances by H^2 and take the limit $H \rightarrow \infty$, which leads to

$$\sigma_I = 0, \quad \sigma_S = \infty, \quad \sigma_{M,\parallel} = \infty, \quad \sigma_{M,\perp} = 1. \quad (12)$$

The definitions (5) and (7) for the exponents s and t are exactly valid only for an infinite system. Instead of using these definitions directly, we adopted the finite-size scaling approach, as described below. For a finite-size system generated *exactly* at the percolation threshold $p_I = p_S$, the system size $L \times L$ is always smaller than the (infinite) correlation length ξ . From Eq. (3) it follows that such a system behaves like a system at another volume fraction satisfying $|p_I - p_S| \sim L^{-1/\nu}$. Therefore, the average of $g_{sat,i}$ or $g_{nonsat,i}$ over many such systems should scale as $\langle g_{sat,i} \rangle \sim L^{-t_i/\nu}$ or $\langle g_{nonsat,i} \rangle \sim L^{s_i/\nu}$. (Due to the appearance of percolating samples, the latter average is actually infinite. A finite result

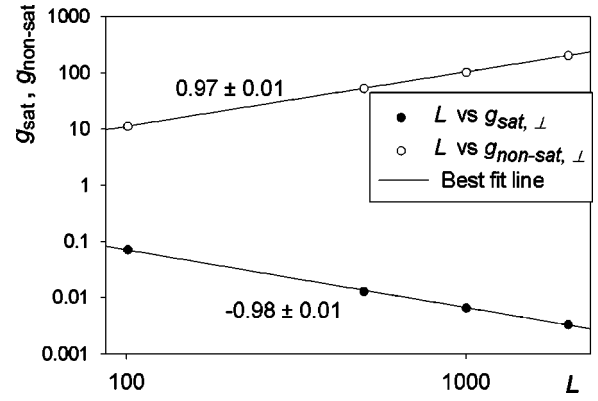


FIG. 3. Calculated $\langle g_{sat,i} \rangle$ and $\langle g_{nonsat,i} \rangle$ [cf. definitions (4) and (6)] plotted on a log-log plot vs linear size L of the RRN for $p_M = 0.2$ and $p_I = p_S = 0.4$. Error bars are smaller than the dot sizes. The slopes of the two lines on this plot equal t_i/ν and $-s_i/\nu$, and are consistent with the value 0.975 , corresponding to $t = s = 1.30$ and $\nu = 4/3$.

is obtained by averaging only over nonpercolating samples. This procedure does not change the scaling form, because *at the percolation threshold* the fraction of samples which are nonpercolating is asymptotically size independent, as discussed below.)

Using RRN's with L ranging from 100 to 2000 and $p_I = p_S$, we estimated s_i and t_i for $p_M = 0.2, 0.5, 0.8$, and, with less accuracy, for several other values of p_M . (At $p_M = 0.8$ we could estimate only t_{\parallel} and s_{\perp} , since these systems usually percolated only in one direction but not in the other.) The finite-size scaling assumption is supported very well, as demonstrated in Fig. 3 for $p_M = 0.2$. Assuming $\nu = 4/3$, we find for all values of p_M studied that $t_{\parallel} = t_{\perp} = s_{\parallel} = s_{\perp} = 1.30 \pm 0.02$. This value supports the hypothesis that the problem belongs to the same universality class as both isotropic and anisotropic percolation in 2D.

The assumption that $\nu = 4/3$ can be tested for our problem by considering percolation in finite-size systems. For such systems, the “percolation threshold” in the direction i is naturally defined as the value of p_S for which exactly one half of the systems percolate in that direction: $P_i \equiv N_{sat,i}/N_{total} = 1/2$, where P_i is the probability of finding saturating behavior in the direction i . Figure 4 then shows that the percolation threshold depends on the system size L . In fact, a finite system has two “percolation thresholds” $p_{S0,\perp}$ and $p_{S0,\parallel}$, located, respectively, above and below the percolation threshold of an infinite system, and approaching p_I as $|p_{S0,i} - p_I| \sim L^{-1/\nu}$ with increasing L .²² We have checked these hypotheses numerically by calculating $|p_{S0,\perp} - p_{S0,\parallel}|$ for four linear sizes L at $p_M = 0.2$ and 0.5 , and verified that $\nu = 4/3 \pm 0.02$, independent of anisotropy.

Figure 4 also makes clear that the fraction of samples which are nonpercolating is size independent at the percolation threshold. Specifically, Fig. 4 shows the fraction of percolating samples of a given size versus concentration p_S . The lines corresponding to different sample sizes L intersect at the percolation threshold $p_I = p_S$ (vertical line). Thus, as $L \rightarrow \infty$, the fraction of the samples percolating at $p_I = p_S$ approaches a certain limiting value determined by the other

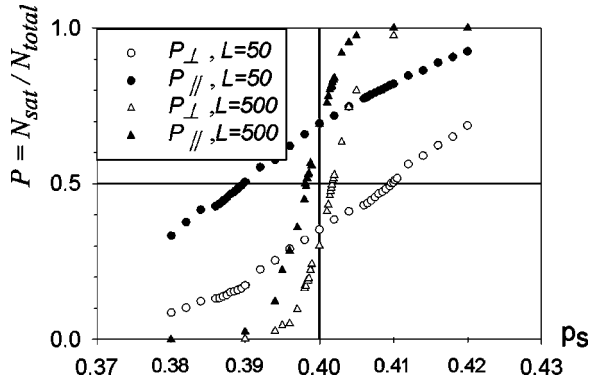


FIG. 4. Fraction $P_i \equiv N_{sat}/N_{total}$ of samples which saturate in the direction i , plotted vs S volume fraction p_S , at fixed M volume fraction $p_M = 0.2$, for two different sizes L . The vertical line denotes the percolation threshold in an infinite system, as predicted by Eq. (2). For a finite system, the “percolation threshold” is the point where one half of the samples percolate: $P_i = 0.5$. Such thresholds are unequal in the directions parallel and perpendicular to \mathbf{B} , but approach the same infinite-size value, $p_{S0} = 0.4$, as $L \rightarrow \infty$.

parameters of the system, namely, the direction of percolation and the concentration p_M of the metal. This limiting value can be related to the spanning probability in the case of *isotropic* percolation in a system of rectangular shape, which was found to depend on the aspect ratio of the rectangle.²³ In the present paper, we only consider systems with the aspect ratio equal to unity; however, the *correlation lengths* are different in the two directions. Thus, $\xi_{\perp}/\xi_{\parallel}$ may be thought of as an effective aspect ratio for the present problem.

In order to test the scaling behavior at finite values of H and Δp , we also simulated random networks at $p_S = p_I$ with large but finite values of both H and L . Since the RRN’s required for such calculations contain bonds with widely different conductivities [cf. Eq. (1)], special care must be taken when performing these calculations on large systems.²⁴ For that reason we wrote special code for storing numbers as large (small) as roughly $10^{\pm 6 \times 10^8}$. Using this code, we studied RRN’s of size up to 4000×4000 in fields ranging from 0 up to $H^2 = 10^8$. One useful way to exhibit those results is as plots of $\ln[(H^2+1)\sigma_{e,i}]$ vs $\ln(H^2+1)$ for different values of the linear size L —see Figs. 5 and 6. Figure 6 shows $\sigma_{e,\parallel}$ and $\sigma_{e,\perp}$ versus magnetic field in systems with sizes ranging from 100 to 4000. For the larger systems, one can clearly see a “critical” range of fields, in which the magnetoresistance is consistent with the scaling form of Eq. (8) with $\delta_{\perp} = \delta_{\parallel} = 1.00 \pm 0.07$. For fields within and below that critical range, the behavior of $\sigma_{e,i}$ is independent of L and is also independent of whether its value does or does not saturate at higher fields, as demonstrated in Fig. 5. However, the intercepts of those linear dependencies are different for the different directions: $\sigma_{e,i} \sim (|H| - H_{0,i})^{\delta_i}$, with positive $H_{0,\perp}$ and negative $H_{0,\parallel}$. This is due to the fact that the system always conducts better in the direction parallel to the applied magnetic field, as can be surmised from Eq. (1). Figures 5 and 6 bear out the forms hypothesized earlier for $F_i(Z)$ —see Eq. (10). In particular, Fig. 5 bears out the expectation that, for small $|Z|$, $F_i(-Z) = -F_i(Z)$, and thus that the scaling func-

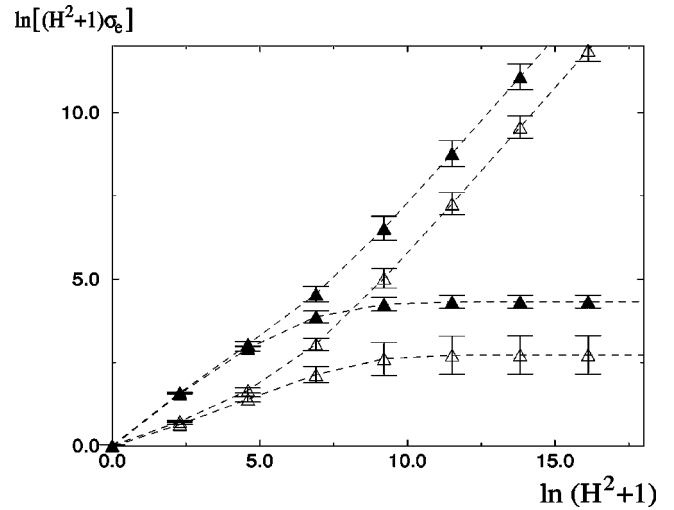


FIG. 5. $\ln[(H^2+1)\sigma_{e,i}]$ vs $\ln(H^2+1)$ for systems with $L = 100$ and $p_M = 0.5$ at the percolation threshold $p_I = p_S$. Averaging over different realizations is performed separately for saturating and nonsaturating samples. Open symbols correspond to $\sigma_{sat,\perp}$ and $\sigma_{nonsat,\perp}$ and the solid symbols to $\sigma_{sat,\parallel}$ and $\sigma_{nonsat,\parallel}$. For values of H within and below the “critical” range of fields (as defined in the text), the conductivity in a given direction does not depend on whether or not it saturates at stronger fields H .

tions are smooth at $Z = 0$. Figures 5 and 6 also show that both $\sigma_{e,\parallel}$ and $\sigma_{e,\perp}$ are independent of L when $|H| \ll L^{1/\nu}$, in agreement with Eqs. (10) and (13) below.

In order to find the form of the scaling functions $F_i(Z)$ [defined by Eq. (9)] from these numerical results, it is con-

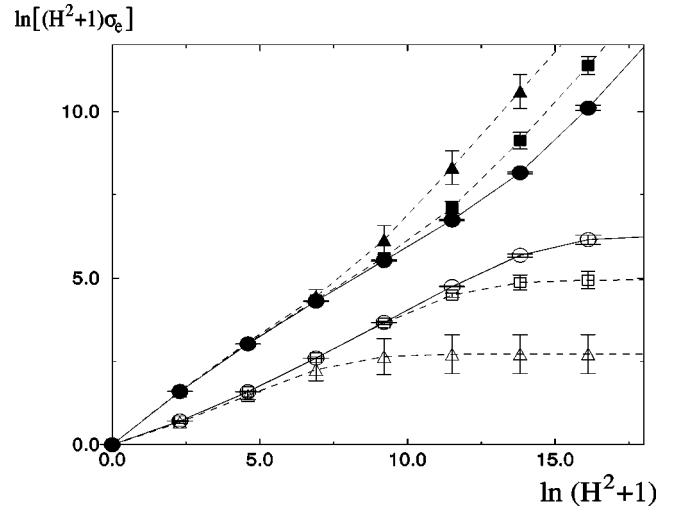


FIG. 6. $\ln[(H^2+1)\sigma_{e,i}]$ vs $\ln(H^2+1)$ for systems of size $L = 100$ (triangles), 1000 (squares), and 4000 (circles), with $p_M = 0.5$, $p_I = p_S = 0.25$. Open symbols correspond to $\sigma_{e,\perp}$ and the solid symbols to $\sigma_{e,\parallel}$. The lines are drawn as guides for the eye. At large fields, all systems exhibit either saturating ($H^2\sigma_i \sim H^2$) or nonsaturating ($H^2\sigma_i \sim 1$) magnetoresistance. In the “critical” range of fields, clearly seen for the larger systems, the magnetoresistive behavior is given by Eq. (8) with $\delta_{\perp} = \delta_{\parallel} = 1.00 \pm 0.07$. Note that, for the sake of visual clarity, we include only those systems in which $\sigma_{e,\perp}$ does not saturate and $\sigma_{e,\parallel}$ does saturate (cf. Fig. 5).

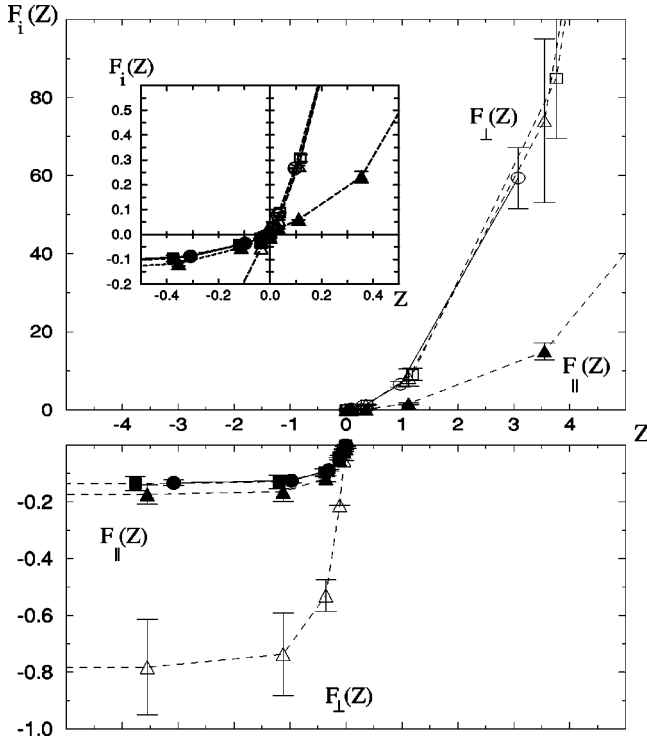


FIG. 7. Plots of $F_i(Z) \equiv \text{sgn} \Delta p L^{-t/\nu} \rho_{e,i} / \rho_{M,\parallel}$ vs $Z \equiv \text{sgn} \Delta p |H| L^{-1/\nu}$ for networks with $p_M = 0.5$ and various large but finite values of H and L . The top frame shows $F_i(Z)$ in the nonsaturating regime, when $Z > 0$, while the bottom frame shows $F_i(Z)$ in the saturating regime, when $Z < 0$. The shapes of the points correspond to the value of L , as in Fig. 6. Open symbols correspond to $F_{\perp}(Z)$, while solid symbols correspond to $F_{\parallel}(Z)$. The horizontal lines surrounding the symbols are parts of error bars. Inset: expanded view of $F_i(Z)$ for small values of $|Z|$ and both signs of Z , showing the smooth linear behavior of $F_i(Z)$.

venient to also invoke the finite-size-scaling hypothesis:²¹ In a system of finite linear size L , when the correlation length ξ satisfies $\xi \gg L$, $|\Delta p|$ should be replaced by $C_1/L^{1/\nu}$ in all the expressions of Eq. (9):

$$\frac{\rho_{e,i}}{\rho_{M,\parallel}} \cong L^{t/\nu} \text{sgn} \Delta p F_i(Z), \quad Z \equiv \text{sgn} \Delta p |H| / L^{1/\nu}. \quad (13)$$

Note that the constant C_1 has been absorbed into the definitions of Z and $F_i(Z)$. The sign of Δp , appearing in Eq. (13), should now be determined from the actual behavior (i.e., percolating versus nonpercolating or saturating versus nonsaturating, in the direction i) of *each particular sample*.

The plots of $\text{sgn} \Delta p L^{-t/\nu} \rho_{e,i} / \rho_{M,\parallel}$ vs $\text{sgn} \Delta p |H| / L^{1/\nu}$, shown in Fig. 7, clearly demonstrate that the results obtained for $\rho_{e,i}$, using different values of H and L , collapse onto a single curve (for a given i) when scaled in accordance with Eq. (13). These figures constitute a quantitative graphical representation of the scaling functions $F_{\parallel}(Z)$ and $F_{\perp}(Z)$ for the special case $p_M = 0.5$. Note that these two scaling functions appear to have a similar shape, up to a constant multi-

licative coefficient. That is qualitatively consistent with the results of the EMA, which lead to⁹

$$\frac{F_{\perp}(Z)}{F_{\parallel}(Z)} = \left(\frac{1 + p_M}{1 - p_M} \right)^2.$$

In the case of the systems featured in Fig. 7, where $p_M = 0.5$, this ratio should be 9 according to the EMA. By contrast, the simulation results plotted in that figure indicate that this ratio is between 4.5 and 5. As stated earlier, such quantitative discrepancies should come as no surprise, in view of the known deficiencies of the EMA in the critical region near a percolation threshold.

V. DISCUSSION

We have demonstrated that the phase diagram of an $M/I/S$ random columnar composite in an in-plane magnetic field exhibits a critical line between saturating and nonsaturating regimes of magnetoresistance. The behavior near this critical line was interpreted using an anisotropic percolation model. The critical exponents $t = s$ and ν were found, numerically, to be the same as in the more conventional 2D isotropic random percolating networks. Also found were the exponents which govern the dependence on magnetic field in the critical region. The existence of scaling behavior in that region was confirmed and the forms of the scaling functions were obtained numerically.

The critical line discussed here could be studied experimentally using a doped semiconductor film as the M constituent, with a random collection of etched perpendicular holes as the I constituent, and a random collection of perpendicular columnar inclusions, made of a high-conductivity normal metal, playing the role of S . Extremely low temperatures or very clean single crystals would not be required in order to observe this critical line. What would be necessary is a large contrast at each stage of the following chain of inequalities $\rho_S \ll \rho_M \ll H^2 \rho_M \ll \rho_I$. If Si-doped GaAs is used as the M host, with a negative charge carrier density of $1.6 \times 10^{18} \text{ cm}^{-3}$ and a mobility $\mu = 2500 \text{ cm}^2/\text{V s}$ at a temperature of 90 K, as in the experiment described in Ref. 3, then a magnetic field of 40 T would result in $H = -10$. Such a material would have an Ohmic resistivity of $1.6 \times 10^{-3} \Omega \text{ cm}$, about 1000 times greater than that of Cu. Thus, using Cu for the S inclusions and etched holes for the I inclusions, all the above inequalities could be satisfied without difficulty.

This is apparently the first experimentally accessible and technologically promising system in which anisotropic percolation is relevant. Our numerical results for the exponents ν , t , s , and δ are consistent with the assumption that this problem belongs to the same universality class as the usual 2D isotropic percolation problem and confirm that ν is independent of anisotropy.

ACKNOWLEDGMENTS

We are grateful to Y. Kantor for providing us with the idea regarding the L dependence of P_i and the appropriate refer-

ences. This work was supported in part by NSF Grants No. DMR97-31511 and DMR01-04987, and by grants from the U.S.-Israel Binational Science Foundation and the Israel Science Foundation.

-
- ¹D.J. Bergman and Y.M. Strelniker, Phys. Rev. B **60**, 13 016 (1999).
- ²D.J. Bergman and Y.M. Strelniker, Phys. Rev. B **49**, 16 256 (1994); **51**, 13 845 (1995); **59**, 2180 (1999).
- ³M. Tornow, D. Weiss, K. von Klitzing, K. Eberl, D.J. Bergman, and Y.M. Strelniker, Phys. Rev. Lett. **77**, 147 (1996).
- ⁴D.J. Bergman and D. Stroud, Solid State Phys. **46**, 178 (1992).
- ⁵P.M. Kogut and J.P. Straley, J. Phys. C **12**, 1 (1979).
- ⁶A.K. Sarychev, D.J. Bergman, and Y.M. Strelniker, Phys. Rev. B **48**, 3145 (1993).
- ⁷M.F. Sykes and J.W. Essam, Phys. Rev. Lett. **10**, 3 (1963).
- ⁸D.J. Bergman, Phys. Rev. B **62**, 13 820 (2000).
- ⁹D.J. Bergman, Phys. Rev. B **64**, 024412-1 (2001).
- ¹⁰For example, in the limit $p_M \rightarrow 1$, the RRN version of the composite at $H \rightarrow \infty$ becomes a set of one-dimensional parallel “wires” composed of $\sigma_{M,\parallel}$ and σ_S bonds. These wires will be broken by σ_I bonds into units with average length a/p_I . These longitudinal wires will be connected by an average of one transverse σ_S bond of length a to neighboring wires (here a is the size of a single bond). As a critical point is approached, since the σ_I and σ_S bonds appear with *equal probabilities*, the size of a critical cluster will grow in both directions in a similar fashion.
- ¹¹A.K. Sarychev and A.P. Vinogradoff, J. Phys. C **12**, L681 (1979).
- ¹²H. Nakanishi, P.J. Reynolds, and S. Redner, J. Phys. A **14**, 855 (1981).
- ¹³M.P.M. den Nijs, J. Phys. A **12**, 1857 (1979).
- ¹⁴B. Derrida and L. De Seze, J. Phys. (Paris) **43**, 475 (1982).
- ¹⁵P.M. Castro de Oliveira, Phys. Rev. B **25**, 2034 (1982).
- ¹⁶D. Arovas, R.N. Bhatt, and B. Shapiro, Phys. Rev. B **28**, 1433 (1983).
- ¹⁷R. Fogelholm, J. Phys. C **13**, L571 (1980); J.-M. Normand, H.J. Herrmann, and M. Hajjar, J. Stat. Phys. **52**, 441 (1988).
- ¹⁸D.J. Frank and C.J. Lobb, Phys. Rev. B **37**, 302 (1988).
- ¹⁹P. Grassberger, Physica A **262**, 251 (1999).
- ²⁰S. Feng, B.I. Halperin, and P.N. Sen, Phys. Rev. B **35**, 197 (1987).
- ²¹A. Aharony and D. Stauffer, *Introduction to Percolation Theory*, 2nd ed., (Taylor & Francis, London, 1992).
- ²²P.J. Reynolds, H.E. Stanley, and W. Klein, Phys. Rev. B **21**, 1223 (1980); M.E. Levinshtein, B.I. Shklovskii, M.S. Shur, and A.L. Efros, Zh. Éksp. Teor. Fiz. **69**, 386 (1975) [Sov. Phys. JETP **42**, 197 (1976)].
- ²³J.L. Cardy, J. Phys. A **25**, L201 (1992); J.-P. Hovi and A. Aharony, Phys. Rev. E **53**, 235 (1996); R.P. Langlands, C. Pichet, Ph. Pouliot, and Y. Saint-Aubin, J. Stat. Phys. **67**, 553 (1992).
- ²⁴Indeed, application of the Y - Δ algorithm (Ref. 18) to such a system leads to generation of intermediary bonds with rapidly growing exponents, both positive and negative. It is important to keep track of such very large and very small numbers, especially in a system that is close to a percolation threshold: a single replacement of a very weak bond by a bond of zero conductance changes the topology of the network, possibly driving it from percolating to nonpercolating.